Nonlinear Optical Properties in Calix[*n*]arenes: Orientation Effects of Monomers

Ayan Datta and Swapan K. Pati*[a]

Abstract: We investigate the nonlinear optical (NLO) polarizations for various geometric arrangements of the dipolar chromophores in a calix[*n*]arene geometry. The interactions were studied by using $(HF)_3$ as model compounds both in parallel and frustrated orientations. The interdipolar angle between the monomer molecules is varied so that many different arrangements of the dipoles can be realized which is associated with the opening up of the calix[*n*]arene rings. Quantum-chemical calculations at both ab initio and semiempirical levels, show that the all-parallel arrangement of the dipoles exhibit the maximum magnitude for the nonlinear optical coefficients at small interdipolar angles for all interdipolar distances. In the frustrated orientations however, the NLO response is maximum at large interdipolar angles corresponding to the flattened calix[*n*]arene rings. The role of hydrogen bonding in stabilizing these assemblies in various conformations has been investigated. Crystallographic database analysis for calix[3]arenes shows that optical properties in real molecular systems can be modeled based on our simple interaction theory.

Keywords: ab initio calculations · calixarenes · crystal engineering · dipole–dipole interactions · nonlinear optics

Introduction

Nonlinear optics has emerged as a topic of great current interest because of its potential applications in lasers, optoelectronic devices and optical limiting processes.[1] A substantial amount of the present research is thus directed towards selection of materials and molecules which exhibit large nonlinear optical properties (NLO).[2] The factors that govern the response of these materials to the applied electric field have been studied quite extensively over the last few decades from a microscopic point of view.[3] With the rapid development in efficient quantum-chemical algorithms and computational power, it is now possible to perform highly accurate calculation of the NLO properties for very large molecules.

In general, molecules having large permanent dipole moment are suitable for strong second-order optical processes such as second harmonic generation (SHG), optical rectification and electrooptic Pockels effect. For these molecules, the electric field induced dipole moment is also very large and thus the difference between the ground state dipole moment and the excited state dipole moment is quite high. In this context, the most preferred systems for NLO active materials are the organic π-conjugated molecules, since the π electrons are more polarizable than the localized σ electrons.[4]

However, the molecular second-order optical polarizability, β, as well as the bulk second-order susceptibility for materials, $\chi^{(2)}$, being a tensor of rank 3, disappear for systems with center of symmetry. Molecules having a substantial ground state dipole moment and thus having large molecular NLO responses have a preferential antiparallel orientation in the molecular crystals. Thus, most often, although the constituent molecules of the crystals are NLO active, their arrangements in the crystalline form make the crystal nonsuitable for NLO device integration.[5] While there has been a lot of effort to understand the microscopic NLO coefficients such as α, β and γ, a proper understanding of the factors governing the bulk susceptibilities of a crystal or in a supramolecular assembly is still elusive.[6] The seemingly weak intermolecular forces as the dipole–dipole interactions, hydrogen bonding,[7] however, play profound roles in governing the overall activity in a macromolecular aggregate.

Noncentrosymmetricity in assemblies can be incorporated: a) by inclusion of chiral centers in the molecules and

[a] A. Datta, Dr. S. K. Pati
Chemistry and Physics of Materials Unit
and Theoretical Sciences Unit
Jawaharlal Nehru Centre for
Advanced Scientific Research Jakkur Campus
Bangalore 560 064 (India)
Fax: (+91) 80-220-82766
E-mail: pati@jncasr.ac.in

 DOI: 10.1002/chem.200401205

also by selection of octupolar molecules or molecules such as 3-methyl-4-nitropyridine-1-oxide (POM) that do not have a ground state dipole moment and have substantial optical responses due to higher order moments.[8] b) Self-assembled monolayers where the individual dipoles are connected in 1-dimensional arrays through phosphate or zirconate units or through hydrogen-bonding interactions.[9]

Much effort has been directed towards the synthesis of calix[*n*]arenes in the last decade.[10] In these class of systems, the individual chromophores are arranged in the form of "baskets" by connecting the constituent molecules by linkers such as $(CH_2)_n$ or $(CH_2O)_n$. Thus, these compounds provide an innovative way of arranging the chromophores in a parallel arrangement.[11] Moreover, one can even increase the number of chromophores in such an assembly by changing "*n*". The interdipolar angle can be varied by functionalizing the lower and upper rims of the "baskets" with groups of different sizes. The overall structure is then controlled by steric classes of interactions. It would thus be very interesting to ask how the individual dipoles of the chromophores interact in such a multi-molecular assembly and how such interactions and molecular properties translate into controlling the overall NLO properties of the calix[*n*]arenes. Although there has been a substantial effort in NLO characteristics of calix[*n*]arenes,[12] a proper understanding from a molecular viewpoint is clearly missing. To our knowledge, there has been only one work to model the NLO properties of these systems,[13] which, however, addresses none of the issues discussed above.

In this paper, we have modelled the NLO properties in calix[3]arenes by studying the dipolar interactions in a similar geometrical arrangement for a hydrogen fluoride trimer, $(HF)_3$. The dipole interaction is varied by i) changing the interdipolar angle amounting to opening up of the "baskets" and ii) increasing the interdipolar distance. Additionally, since the most favorable arrangement for any dipolar system is the antiparallel arrangement, we perform similar calculation for such a "frustrated" dipolar system, $(HF)_3$, with two dipoles in the parallel arrangement while the third one in the antiparallel orientation with the other two. For such a "frustrated" arrangement with the basket opening up, a favorable hydrogen-bonding interaction is developed, which further stabilizes the system. Finally, we performed calculations on the calix[3]arenes and compare the results with our model developed for $(HF)_3$ system.

Theory

Geometry of the model $(HF)_3$ system: Three HF molecules are arranged parallel to each other so that the lower base (lower rim) has three H atoms and the upper base (upper rim) has three F atoms. The three H and the three F atoms in each rim form two equilateral triangles. The geometry is shown in Figure 1a. This is the all-parallel arrangement for the dipoles, applicable for a parallel cylindrical arrangement as in calix[*n*]arenes.

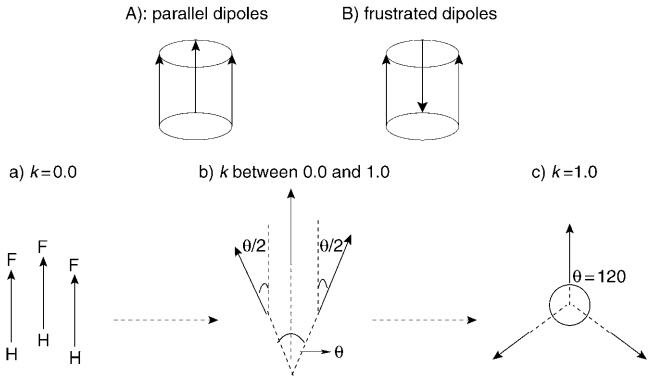

Figure 1. Arrangement of dipoles in a basket-type geometry for A) parallel and B) anti-parallel geometries. a) Parallel dipoles with interdipolar angle, $\theta = 0°$; b) geometry as the dipoles open up, the lower rim radius remains constant and the upper rim radius changes; c) fully opened basket with interdipolar angle, $\theta = 120°$.

However, the most stable arrangement of such a dipolar arrangement is the antiparallel arrangement. Systems such as calix[4]arene have a significant percentage of the antiparallel form (u,d,u,d; u,u,d,d) apart from the all-parallel cone geometry (u,u,u,u or d,d,d,d).[14] Such a relaxation from the all-parallel to the antiparallel arrangement is possible only for calix[*n*]arenes with even number of chromophores, $n = 4$, 6, 8 and so on. For odd number of dipoles in the assembly, such a relaxation is, however, not possible. For example, for $n = 3, 5, 7$ and so on the dipoles are in a *frustrated* arrangement where the overall dipole moment for the relaxed geometry does not vanish. The individual chromophores in calix[*n*]arenes are connected by short bridges that prevent random orientations of the dipoles. The simplest of such an arrangement is the $(HF)_3$ system shown in Figure 1b. In fact, the $(HF)_3$ system is the simplest case for a molecular assembly that can be studied for both parallel and frustrated cases simultaneously.

The interdipolar angle for real molecular systems is controlled by the steric bulk of the groups on the lower and the upper rim of the cylinder. An increase in bulkiness of the groups in the upper rim while keeping the steric bulk of the lower rim constant, increases the interdipolar angle with opening up of the basket. Thus, the system having a cylindrical symmetry is converted into a conical-shaped geometry.

For modeling the opening up of the cylinder for both the parallel (A) and frustrated dipoles (B), we keep the lower rim with corresponding three atoms constant and vary the coordinates of the three atoms in the upper rim. The radius of the upper rim can be increased by translating the corresponding atomic coordinates according to: $X = X+kX$, $Y = Y+kY$ and $Z = Z-kZ$, while keeping all the three molecular (HF) bond lengths fixed. The Z axis corresponds to the internuclear axis and k is the flattening parameter which varies from 0 to 1.0. While the $k = 0$ case corresponds to the perfect cylindrical arrangement for an interdipolar angle $\theta = 0°$ [see Figure 1a], the $k = 1.0$ signifies the other extreme where the cylinder becomes completely flat (Z coor-

dinates are zero) so that all the six atoms (3H and 3F) are on the same plane, forming a circular disk. For such a case ($k=1.0$), the interdipolar angle $\theta=120°$ [see Figure 1c]. For all intermediate values of k, between 0.0 to 1.0, the cylinder is progressively opened and the interdipolar angle, θ, increases from 0 to 120° [see Figure 1b].

Ground state dipole moment: With the dipoles opening up, the total ground state dipole moment changes as a function of the interdipolar angle. A general dipole moment expression for the combined effect of three dipoles can be written as Equation (1):

$$\mu_G = \sqrt{\mu_a^2 + \mu_b^2 + \mu_c^2 \pm 2\mu_a\mu_b\cos\theta_{ab} \pm 2\mu_b\mu_c\cos\theta_{bc} \pm 2\mu_c\mu_a\cos\theta_{ca}} \quad (1)$$

where μ_a, μ_b and μ_c are the dipole moment vectors for three dipoles *a*, *b*, *c* and θ_{ab}, θ_{bc} and θ_{ca} represent the angles between the corresponding dipoles. Note that the dipolar angle determines the phase (+ve for parallel and −ve for frustrated arrangement) of the dipoles.

For the present case when all the dipoles are same (homomolecular system), $\mu_a = \mu_b = \mu_c = \mu_i$ and $\theta_{ab} = \theta_{bc} = \theta_{ca} = \theta_{ij}$. In the parallel orientation (A), all the vectors are in-phase. Thus, the total dipole moment is given by Equation (2):

$$\mu_G = \sqrt{3\mu_i^2 + 6\mu_i^2\cos\theta_{ij}} \quad (2)$$

For $\theta_{ij} = 0°$, the μ_G has a maximum value of $3\mu_i$. When θ_{ij} increases from 0 to 120°, the μ_G decreases monotonically to zero.

In the frustrated arrangement (B), two of the interdipolar angles are out-of-phase and one of them is in-phase. Thus the total dipole moment is given in Equation (3):

$$\mu_G = \sqrt{3\mu_i^2 - 2\mu_i^2\cos\theta_{ij}} \quad (3)$$

For this geometry, the μ_G increases from μ_i (for $\theta_{ij} = 0°$) to $2\mu_i$ (for $\theta_{ij} = 120°$). Thus, for such a frustrated dipolar system, the ground state dipole moment is a monotonically increasing function of the interdipolar angle.

Excitonic splitting for a multidipolar aggregate: The above expressions for the dipole moments are purely classical without any correlation among the dipoles. However, for systems with nonzero ground state dipole moment, there exists a strong dipole–dipole interaction. This dipole–dipole interaction leads to a large excitonic coupling and the effects are most prominent in the excited state of the molecules.[15–20] A Scheme of interaction between the three dipolar molecules is shown in Figure 2. For such an aggregate, while the ground state, G[$|G\rangle = |g_1g_2g_3\rangle$] is stabilized with respect to the monomer ground states, the excited states which remain degenerate at infinite distance between the monomers, undergo splitting into three states, (E_1 [$|E_1\rangle = 2|e_1g_2g_3\rangle - |g_1g_2g_3\rangle - |g_1g_2g_3\rangle$], E_2 [$|/E_2\rangle = |g_1e_2g_3\rangle - |g_1g_2e_3\rangle$] and E_3 [$|E_3\rangle = |e_1g_2g_3\rangle + |g_1e_2g_3\rangle + |g_1g_2e_3\rangle$]), when they are brought closer (see Figure 2). Interestingly, out of these three states, two states (E_1 and E_2) are degenerate while E_3 is nondegenerate and symmetric. The extent of splitting, ΔE, however, depends on the strength of dipole–dipole interactions, given by Equation (4):

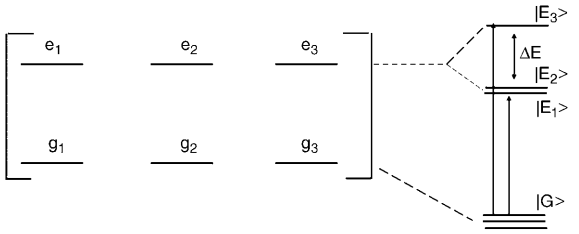

Figure 2. Excitonic splitting in a trimolecular dipolar aggregate due to dipole–dipole interactions. $|G\rangle$ and $|E_1\rangle$, $|E_2\rangle$, $|E_3\rangle$ represent the unnormalized eigenfunctions for the ground and excited states, respectively, in the assembly. Each $|g_ig_je_k\rangle$ is a direct product state of the aggregate involving the monomer states $|g_i\rangle$, $|g_j\rangle$ and $|e_k\rangle$ of the monomers *i*, *j* and *k*, respectively.

$$\Delta E = \sum_{i,j} 2\frac{M_{gs}^2}{r_{ij}^3}(\cos\theta_{ij} - 3\cos^2\psi_i) \quad (4)$$

where M_{gs} is the transition dipole from the ground state to the excited singlet state of the monomer, r_{ij} is the interdipolar distance between the molecules *i* and *j* and the summation index is over all the three molecules. The aggregate is constructed such that the orientation angle between any two monomers is θ_{ij} [$\theta_{ij} = \theta_{12} = \theta_{23} = \theta_{31} = \theta$] and each monomer creates an angle ψ with its molecular axis [also $\psi_i = \psi_1 = \psi_2 = \psi_3 = \psi$].[21] From the above expression it is evident that a singlet excited state of the monomer molecule would split according to the intermolecular angles (θ) and molecule-dipole angles (ψ). For linear molecules or donor–π–acceptor type chromophores with a *para* orientation (e.g. *para*-nitroaniline), the dipolar axis and the molecular axis are collinear and thus $\psi=0°$.

With the increase in the inter-monomer angle corresponding to the flattening up of the basket, there is a variation in the oscillator strength in the three states, E_1, E_2 and E_3. For the parallel case, at $\theta=0$, E_3 is the only dipole allowed state with large oscillator strength, since it corresponds to the *in-phase* combination of all the three dipoles. However, as the interdipolar angle increases, in addition to E_3, E_1 and E_2 also become dipole allowed, more so for large flattening angle. For the frustrated assembly however, all the states are dipole allowed at $\theta=0$ and as θ increases, the E_1 and E_2

become strongly allowed (higher oscillator strength) while E_3 becomes progressively weaker.

Results and Discussions

We started our calculations by calculating the dipole moment and the equilibrium ground state bond length for hydrogen fluoride (HF). We have taken into account substantial amount of electron correlation by two different methods: The Becke's three parameterized hybrid DFT method (B3LYP) and the MP2 methods.[23,24] In order to compare the effects of electron-correlation as well as basis set effects, we have varied the level of basis set from the 6-31G to aug-cc-pVQZ for both the two methods. They are shown in Table 1. The experimental values for the R_{eq} and dipole moment of HF are 0.920 Å and 1.80 Debye, respectively.[25] Thus, the B3LYP at a large basis-set of aug-cc-pVQZ can reproduce the experimental parameters very well and we select the dipole moment of HF, μ(HF) = 1.8084 Debye for all further calculations.

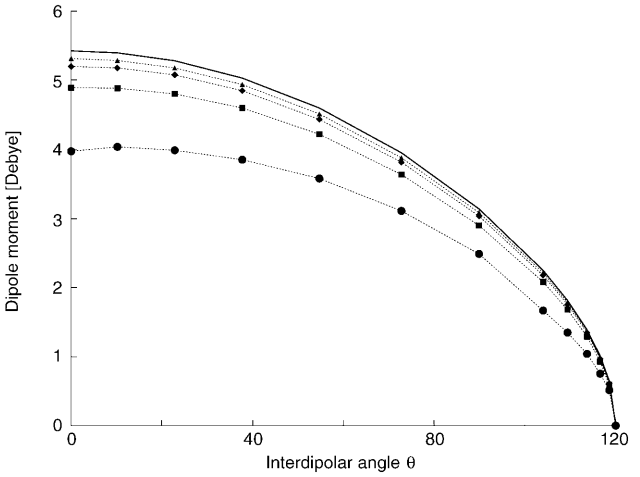

Figure 3. μ_G as a function of the interdipolar angle, θ for the parallel dipolar assembly; interpolar distance d: ▲ 4.5, ◆ 3.5, ■ 2.5, ● 1.5 Å, —— analytical.

Table 1. The bond length [Å] and dipole moment [Debye] for HF for different level of basis sets and different methods.

Basis set	B3LYP		MP2	
	bond length	dipole moment	bond length	dipole moment
6-31G	0.94926	2.150	0.94700	2.3368
6-31G(d,p)	0.95202	1.8277	0.92142	1.9800
6-31G++(d,p)	0.92788	1.9913	0.92650	2.0888
6-311G	0.93945	2.2155	0.93666	2.3588
6-311G(d,p)	0.92008	1.9023	0.91289	2.0118
6-311G++(d,p)	0.92216	1.9818	0.91668	2.0662
cc-pVQZ	0.92142	1.8239	0.91715	1.9339
aug-cc-pVQZ	0.92216	1.8084	0.91861	1.9255

In the previous section, we have derived the expression for the total ground-state dipole moment, μ_G as a function of the interdipolar angle. Since it does not include any correlation effect, we have calculated the ground-state dipole moment for the $(HF)_3$ assembly at various interdipolar angles using the B3LYP//aug-cc-pVQZ method. The variation of the dipole moment with the interdipolar angle for the all-parallel geometry of the dipoles (case A in Figure 1) is plotted in Figure 3. The interdipolar distances (d) are varied from 1.5 to 4.5 Å. For comparison, the same plot for the analytical classical dipole moment is also shown.

At small interdipolar distances like 1.5 Å, the computed dipole moment shows a very large deviation from the non-interacting analytical value. For example, at $\theta = 0°$, the magnitude of the total dipole moment is only 3.9721 Debye compared with the analytical 5.4252 Debye, a reduction of 27%. But, as the basket opens up, the deviation decreases and both the computed and the analytical values converge to 0 Debye for $\theta = 120°$. This signifies the role of electronic correlations for the $(HF)_3$ assembly at small interdipolar distances and small interdipolar angles. But, as the interdipolar distance (d) between the HF monomers increases (around d ~4.5 Å), the intermolecular interaction decreases and the system transforms into a classical dipolar assembly, so that the classical expression for the dipole moment remains valid at large interdipolar distances.

The variation of μ_G for the frustrated dipolar system (B) shows very interesting features (see Figure 4). At small interdipolar angles, the calculated dipole moments differ from the classical values particularly at small d. This is similar to the case for parallel dipoles. However, contrary to the parallel dipoles (see Figure 3) where, with increase in the dipolar angle, the deviation becomes less prominent, the frustrated dipolar systems show very large deviation from the classical dipole moment values for large θ. The deviation is the largest for the case of small interdipolar distance of 1.5 Å.

As the basket starts to open up, two of the hydrogen atoms in two HF molecules come close to the fluorine atom of the third HF molecule. Initially the F···H-F angle is 90° but as the dipoles flatten up, the F···H-F angle increases towards 180°. Such a linear F···H-F conformation has been found to be most suitable for the hydrogen-bonding interaction.[26] Therefore, with the increase in the interdipolar angle, the hydrogen-bonding interaction increases. The effect is most profound for the interdipolar distance of 1.5 Å as the F···H–F bond is strongest at such distances. Hydrogen-bonding interaction is primarily electrostatic in nature with δ^- on the F atoms and δ^+ on the hydrogen atoms. Not only the linearity, the distance between the electronegative atom and hydrogen atom also is crucial for effective charge transfer. Therefore, there is an overall enhancement of 30% in the dipole moment magnitude compared with the non-in-

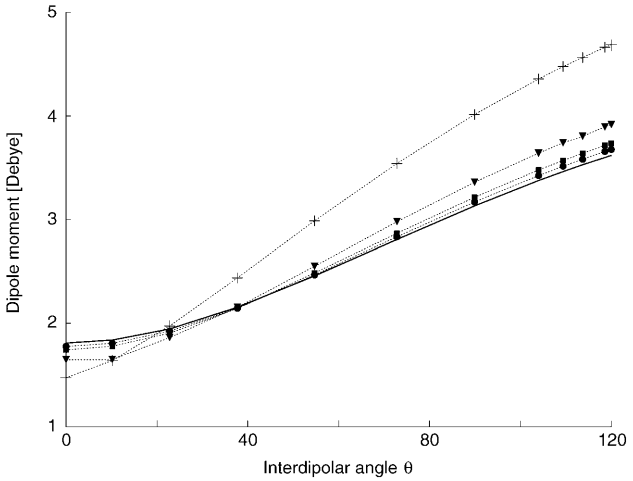

Figure 4. μ_G as a function of the interdipolar angle, θ for the frustrated dipolar assembly; interpolar distance d: ● 4.5, ▼ 3.5, ■ 2.5, + 1.5 Å, —— analytical.

teracting value in the ground state dipole moment at small interdipolar distances and large θ values. However, as the interdipolar distance increases, the H–F···H bond becomes weaker and there is very little enhancement in the dipole moment from the classical value.

From the above discussion it is clear that the extent of exciton splitting as well as the ground state dipole moment depend on the angular orientation of the dipoles. It will be novel to study such effects on the variation of the nonlinear optical properties for such systems.

For a quantitative estimation of the non-linear optical response property such as the 1st hyperpolarizability (β) for the geometries at the various interdipolar angles, we calculate the frequency dependent hyperpolarizability at 1064 nm corresponding to the experimental Nd/YAG frequency using the well-established analytical TDHF formalism with 6-31G-(d,p) basis set.[27] The level for the basis set was varied from 6-31G(d,p) to 6-311G++(d,p) without any significant change in the magnitudes for β. We report below the β values obtained at the level of TDHF/6-31G(d,p).

In Figure 5, we plot the HOMO–LUMO gap as a function of the interdipolar angle for the $(HF)_3$ (all-parallel system, case A, in Figure 1) for a number of interdipolar distances. We have further verified that the HOMO–LUMO gap from TDHF/6-31G(d,p) actually corresponds to the optical gap found from ZINDO-CI calculations (see next Section for a detailed description of the calculations involving ZINDO-CI approach). The optical gap is calculated as the energy difference between the geometry relaxed ground state and the lowest optically allowed state with substantial oscillator strength. This corresponds to the vertical optical absorption gap. We see that for the $(HF)_3$ system at a small interdipolar distance of 1.5 Å, the optical gap is only 14 eV compared to 21 eV for large interdipolar distance, both for a small interdipolar angle, $\theta = 0$. As the interdipolar angle increases, the gap for the small interdipolar distance increases up to $\theta \approx 70°$, after which the optical gap saturates to a value of 21 eV. For larger interdipolar distances of 2.5, 3.5 and 4.5 Å there is no excitonic splitting and the gap remains almost constant at 21 eV. To quantify the extent of splitting in the $(HF)_3$ system, we calculated the optical gap for a single HF molecule. The gap is ≈ 22 eV. But as we have shown, it is possible to reduce the optical gap to 60% of the monomer value in an aggregate. Such a remarkable effect can be realized by only fine tuning the interdipolar distance and the associated phase angle.

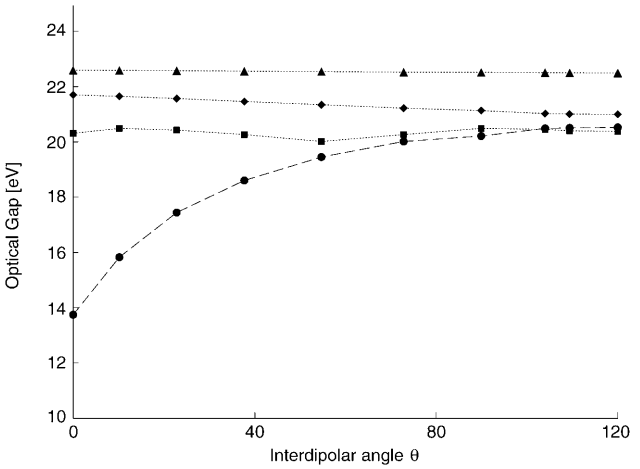

Figure 5. Optical gap as a function of the interdipolar angle, θ for the parallel dipolar assembly at TDHF/6-31G(d,p) level; interpolar distance d: ▲ 4.5, ◆ 3.5, ■ 2.5, ● 1.5 Å.

The same feature is also seen for the frustrated dipolar assembly, shown in Figure 6. The optical gap increases from 16 eV to the monomer (non-interacting) limit of 22 eV after an interdipolar angle of $\approx 70°$. For, larger interdipolar distances, there is no excitonic splitting and the gap remains constant at 22 eV. Note that, for small interdipolar distance of 1.5 eV and for $\theta = 0$, the frustrated case (case B in Figure 1) shows larger gap (16 eV) compared to the all-parallel geometry (A) (14 eV) due to hydrogen-bonding stabilization of the ground state for the former.

We now investigate the variation of the first hyperpolarizability (β) as a function of the interdipolar angle and the distances between them for the parallel orientations. At a small interdipolar distance of 1.5 Å, the magnitude of β decreases very rapidly with the increase in the interdipolar angle till $\theta \approx 30°$ (Figure 7a). After such an initial steep decay, β decreases monotonically and reduces to zero at $\theta = 120$. Thus, the β profile shows a clear signature of two parameters. At smaller interdipolar angles ($\theta < 50°$), it is the optical gap that controls the magnitude of β. In fact, for smaller θ, the plot is similar to the plot for the optical gap (mirror image) which increases and then saturates (see Figure 5). Since the optical gap appears in the denominator in the β expression, the optical gap and the β have an inverse relation, clearly visible by comparing Figures 5 and 7a. At larger interdipolar angles however, when the optical gap

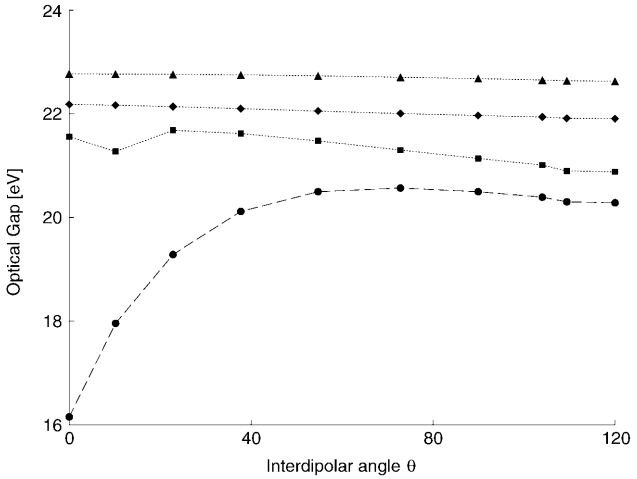

Figure 6. Optical gap as a function of the interdipolar angle, θ for the frustrated dipolar assembly at TDHF/6-31G(d,p) level; interpolar distance d: ▲ 4.5, ◆ 3.5, ■ 2.5, ● 1.5 Å.

almost saturates, the ground state dipole moment (effectively the difference between the ground state and the excited state dipole moment) controls β. This is again clearly seen by comparing Figures 7 and 3.

However, with the increase in the interdipolar distances, the optical gap becomes constant with a large value as in the monomer limit. For such cases, the dipole moment difference between the ground state and the excited state (with the maximum oscillator strength) plays the major role in determining β with the increase in interdipolar distance. This is seen in the Figure 7b. For the interdipolar distance of 2.5 Å, the plot for β shows a monotonic decrease and decays to zero at $\theta=120$. If the optical gap was solely responsible for β, then the graph would have looked flat. A qualitative idea for such a feature can be understood from the two-state model for β. This model assumes that the electronic properties of the molecule are determined by a ground state and a low-energy charge transfer excited state. Polarization results primarily from the mixing of the charge-transfer state with the ground state through the interaction of the molecule with the electric field.[28]

$$\beta_{\text{two-level}} = \frac{3e^2}{2\hbar}\frac{\omega_{12} f \Delta\mu_{12}}{(\omega_{12}^2-\omega^2)(\omega_{12}^2-4\omega^2)} \quad (5)$$

where ω_{12} is the frequency of optical transition between states 1 and 2, f is the oscillator strength and is the square of the transition moment between the ground state and the excited state $\langle 1|er|2\rangle$ and $\Delta\mu_{12}$ is the difference between the ground-state and the excited-state dipole moments. The most important aspect to note from this equation is that the β is directly proportional to $\Delta\mu_{12}$ and inversely proportional to the optical gap.

At large interdipolar distances, optical gap saturates, so that the magnitude of the excitonic splitting is no more important. However, the question remains whether the excitation is more polarizable than the ground state. In fact, we find that it is the $\Delta\mu_{12}$ which governs the magnitude of β at intermediate dipolar angles for large interdipolar distances. The signatures for such dipole moment controlled β is also seen for higher interdipolar distances which also decay monotonically to zero at $\theta=120$. The β value for distances 3.5 and 4.5 Å are shown in Figure 7c and d, respectively, for the parallel dipolar assembly.

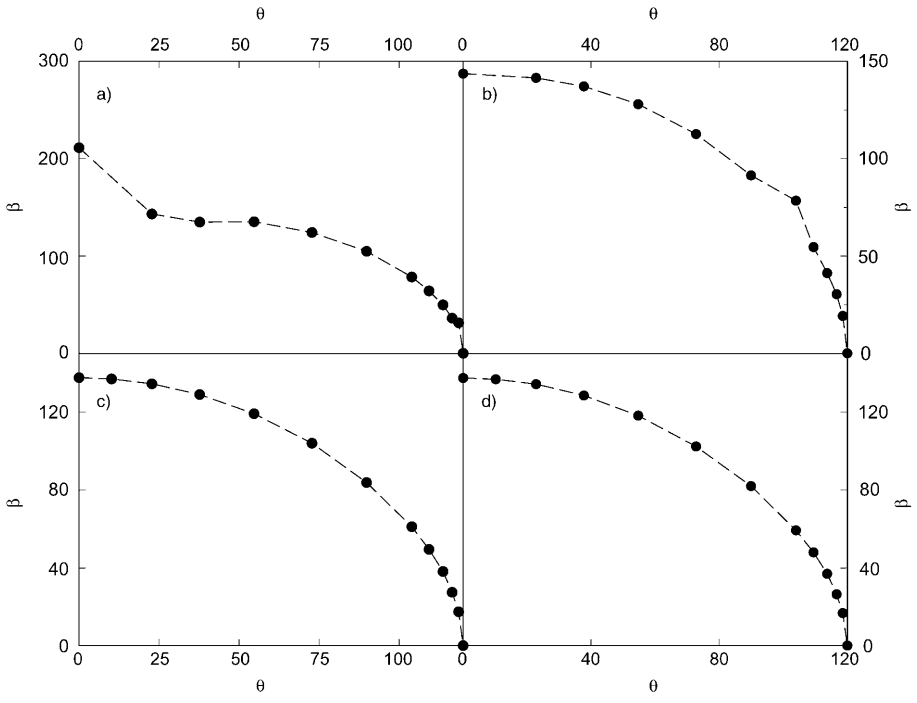

Figure 7. Variation of β with respect to the interdipolar angle at varying interdipolar distance d [a) 1.5, b) 2.5, c) 3.5, d) 4.5 Å] for parallel orientation at TDHF/6-31G(d,p) level. β is in atomic units.

The frustrated dipolar assembly (case B in Figure 1) also exhibit very similar qualitative trends. For a small interdipolar distance of 1.5 Å, β decays with the increase in the interdipolar angle till $\theta \approx 30°$ (Figure 8a). Such a steep decrease is also due to the increase in the optical gap at such interdipolar angles. But after the saturation of the optical gap, β is entirely controlled by the dipole moment which increases with the increase in the dipole moment (Figure 4). At larger interdipolar distance of 2.5 Å (Figure 8b), 3.5 Å (Figure 8c) and 4.5 Å (Figure 8d) where the optical gap saturates, β shows a monotonic

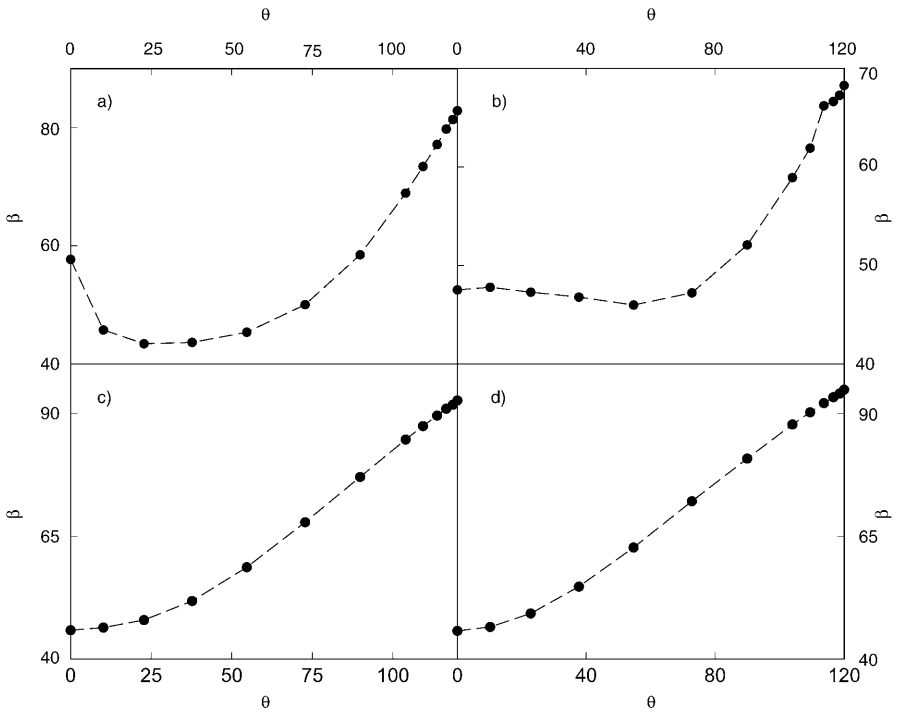

Figure 8. Variation of β with respect to the interdipolar angle at varying interdipolar distance d [a) 1.5, b) 2.5, c) 3.5, d) 4.5 Å] for frustrated orientation TDHF/6-31G(d,p) level. β is in atomic units.

increase with the increase in the interdipolar angle again due to similar features in dipole moment (see Figure 4).

Calix[3]arenes: Until now we have considered the case for a model system of $(HF)_3$ with three dipolar units. Molecular species such as calix[3]arenes have a similar arrangement for the chromophores and by suitable functionalization at either end of these constituent units, these chromophores can be made dipolar. We consider a simple prototype calix[3]arene that can serve as the model for any other higher order ($n > 3$) and more involved examples of such calix[*n*]arenes. Figure 9 shows the two molecules i) and ii) that we have used for calculation. The geometries were optimized at the ab initio level using the B3LYP method at a 6-31G++(d,p) basis set. The geometry optimized synthon, $(CH_3)_3$C-Ph-NO_2, is also shown. We have selected this synthon as the monomer because the steric interaction between the *tert*-butyl groups will prevent the aggregate to flatten. Additionally, three synthons are connected by -CH_2-CH_2-CH_2- units. Such a linker is useful since it is optically inert and does not add any further complexity that an oxo bridge has because of its high electronegativity. Thus the change in the optical properties in the aggregate and the individual monomer can be understood from our model $(HF)_3$ case discussed above.

Figure 9i shows a parallel orientation for the dipoles. As can be seen from the structure, the monomers do not have the same phase angle with each other as the structure relaxes from the exact parallel arrangement to a relaxed geometry. For ii), we consider a similar case of frustrated dipolar geometry that we have discussed earlier in the context of $(HF)_3$. Two of the $(CH_3)_3$C-Ph-NO_2 moieties are parallel while the third one remains anti-parallel to the other two. Energy minimization for the structure leads to a relaxation from the all unidirectional orientation. The dipole moment of the monomer is 5.92 D while the aggregate i) has a dipole moment of 13.1 D. One can calculate the average cone angle, θ_{ij} for such an arrangement using Equation (2), as both μ_G and μ_i are known. We find that for structure i), $\theta_{ij} = 71.57°$. Note that the individual dipoles do not make a uniform angle with respect to each other and thus θ_{ij} is not a uniquely defined angle due to relaxation in the optimized structure. This is true for all the real molecular architectures in calix[*n*]arenes. However, θ_{ij} does provide a very simple "thumb-rule" parameter for defining the cone angle and the dipole interaction for such otherwise complicated geometries. For ii), the net dipole moment for the aggregate is 4.67 D, less than that for a single molecule and the dipolar axis for ii) (seen as a green

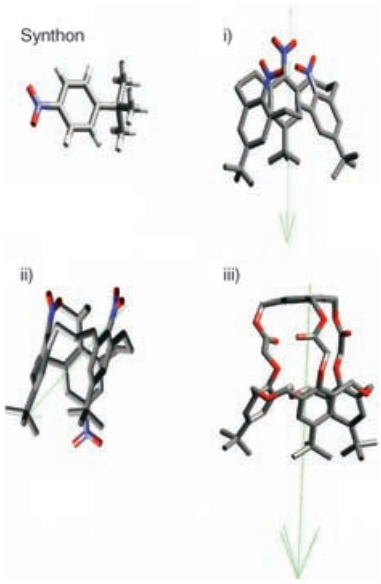

Figure 9. Structure of the synthon, $(CH_3)_3$-Ph-NO_2, i) the all-parallel dipolar aggregate; ii) the frustrated dipolar aggregate; iii) geometry from crystal structure of a molecule in all-parallel arrangement of dipoles. H not displayed in i), ii) and iii) for sake of clarity. The light green arrow shows the direction of the computed dipole moment. Atom colour code: H = white, C = black, N = blue and O = red.

arrow) does not coincide with the cylindrical axis of the geometry. Using Equation (3) for ii), θ_{ij} is found to be 67.80°.

For these molecules, the SCF MO energies and then the spectroscopic properties were computed using the Zerner's INDO method.[29] We have varied the levels of CI calculations, with singles (SCI) and multi-reference doubles CI (MRDCI), to obtain a reliable estimate of the second order optical response functions. The later method is particularly important since it includes correlation effects substantially. The MRDCI approach adopted here has been extensively used in earlier works, and was found to provide excitation energies and dipole matrix elements in good agreement with experiment.[30,31] As reference determinants, we have chosen those determinants which are dominant in the description of the ground state and the lowest one-photon excited states.[32] We report below the MRDCI results with four reference determinants including the Hartree–Fock ground state. For each reference determinant, we use five occupied and five unoccupied molecular orbitals to construct a CI space with configuration dimension of 800 to 900. To calculate NLO properties, we use correction vector method, which implicitly assumes all the excitations to be approximated by a correction vector.[33] Given the Hamiltonian matrix, the ground state wave function and the dipole matrix, all in CI basis, it is straightforward to compute the dynamic nonlinear optic coefficients using either the first order or the second order correction vectors. Details of this method have been published in a number of papers.[34–36] All the calculations have been performed for the frequency 1064 nm corresponding to the Nd/YAG laser.

For the parallel arrangement of the monomers, (structure i in Figure 9) excitonic splitting due to dipole–dipole interactions is substantial, $\Delta\beta$ ($\beta_{molecule} - 3\beta_{monomer}$) = 705 au (see Table 2). Note that there is a large increase of β compared to its monomer value of 7593.2 au, even though interdipolar angle, θ_{ij}, is quite large. However for structure ii, $\Delta\beta$ = −3734.1 au, supporting the fact that dipolar axis and the cylindrical axis do not coincide due to relaxation of the structure.

For a more conclusive comparison of the evolution of the 1st hyperpolarizability with respect to the interdipolar angle, we compute the magnitude of β with the increase in the interdipolar angle, θ_{ij}. This is done by removing the -CH_2-CH_2-CH_2- connectors between the chromophores and then flattening the calix[3]arene similar to that done for $(HF)_3$ (Figure 1). The profile is shown in Figure 10. β shows a monotonic decay with the increase in the interdipolar angle and decays to zero at $\theta = 120$. It is very interesting to note that in Section on Theory we discussed similar features for the

Table 2. Ground state dipole moment (in Debye) and first hyperpolarizability (in atomic units) for individual constituent and their aggregates in calix[3]arene.

Molecule	μ_G	β
$(CH_3)_3$-Ph-NO_2	5.920	7589.727
trimer: parallel	13.093	23474.100
trimer: frustrated	4.670	19035.087
trimer: crystal geometry	6.650	32076.640

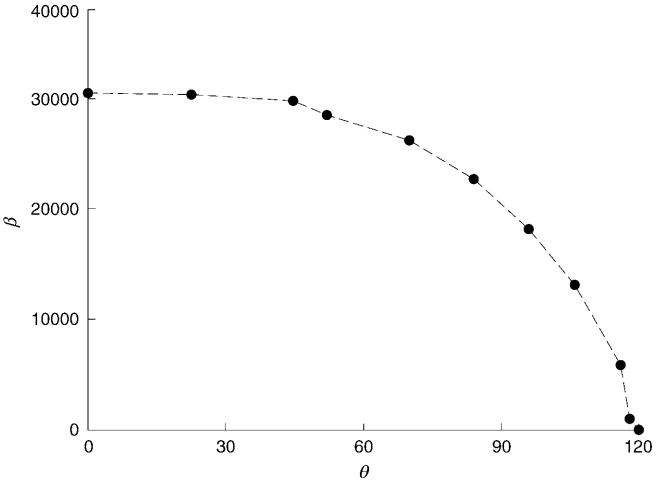

Figure 10. Variation of β with respect to the interdipolar angle at varying interdipolar distance for parallel orientation of the monomers in calix[3]-arene at ZINDO/MRDCI-CV level. β is in atomic units and θ is in degrees.

$(HF)_3$ assembly (Figure 7b–d) in the case of $(HF)_3$ with all-parallel geometry. Thus our $(HF)_3$ model system serves as a very good template for studying interactions in real supramolecular assembly.

CSD search: For high NLO responses, the intermolecular conformation of the dipoles should be parallel or almost parallel. To find out real molecular systems where such a single orientation is possible, we carried a search using the keyword "calix[3]arene" in the Cambridge Structural Database[37] (CSD version, 5.25, November 2003 release). Structures of low quality ($R > 10\%$), disordered or in which the position of H atoms have not been determined were excluded. A total of four structures were retrieved. Of these, two of the structures, CSD code: DIPWEE[38] and QETWAN[39] maintain a parallel-like orientation of the monomer chromophores. These two molecules maintain such a parallel arrangement for two entirely different reasons. DIPWEE has a large cavity size that incorporates a fullerene which prevents crossover to the frustrated dipolar form. However, due to its large cavity, it gives a large angle cone conformation. From our analysis based on the $(HF)_3$ geometry, we have shown that structures with a large cone angle are not suitable for efficient NLO applications. Thus, we did not pursue the NLO calculations for this molecular crystal.

QETWAN, on the other hand is the simplest yet extremely interesting. The structure has been shown in Figure 9iii. It has all the three individual chromophores in the same parallel orientation. The fourth chromophore is functionalized at the *meta*-positions such that it acts as a stitch for the rest of the three and forces a parallel orientation for the dipoles. The light green arrow is the ground state dipole moment axis and it passes almost exactly through the central axis of this basket and thus is very suitable candidate that supports our dipolar model based on $(HF)_3$. The compound has the highest magnitude for the 1st hyperpolarizability among all the systems considered for this work ($\beta = 32076.64$ au).

Conclusions

In this work we have developed an analytical theory for the variation of the ground state dipole moment on the orientation of the dipoles with cyclic boundary conditions. We have proposed the "cone-angle" as a unique parameter by which many interesting states of aggregation can be derived. To the best of our knowledge this is the first comprehensive study on such calix[*n*]arene geometries for NLO applications. Our numerical calculations on the small model dipolar aggregates of $(HF)_3$ (parallel and frustrated cases) show that these analytical expressions are very reliable provided the molecular orbitals of the individual species do not overlap with each other.

Our high level numerical calculations for the optical properties such as β show a very large role of excitonic splitting at small dipolar distances as a result of which β decays very rapidly. At large interdipolar distances however, β shows a monotonic decrease due to similar ground state dipole moment. Our calculations provide the means of finding nonlinear polarizabilities for various cone angles, applicable for real molecular entities as well. Finally, our calculations on calix[3]arenes show that indeed our dipole orientation model is very suitable for studying actual molecular baskets where the conical symmetry is preserved.

Acknowledgements

We thank Prof. Anna Painelli for helpful discussions. S.K.P. thanks CSIR and DST, Govt. of India, for the research grants.

[1] a) Optical Nonlinearities in Chemistry (Ed.: D. M. Burland), *Chem. Rev.* **1994**, *94*, Issue 1 (whole Issue); b) R. Boyd, *Nonlinear Optics*, 2nd ed., Academic Press, **2003**.

[2] a) T. J. Marks, M. A. Ratner, *Angew. Chem.* **1995**, *105*, 167; *Angew. Chem. Int. Ed. Engl.* **1995**, *34*, 155; b) *Nonlinear Optical Materials*, ACS Symposium Series 628 (Eds.: S. P. Karna, A. T. Yeates), Washington DC, **1996**.

[3] a) D. P. Shelton, J. E. Rice, *Chem. Rev.* **1994**, *94*, 3; b) D. C. Hanna, M. A. Yuratich, D. Cotter, *Nonlinear Optics of Free Atoms and Molecules*, Springer, Berlin, **1979**.

[4] P. N. Prasad, D. J. Williams, *Introduction to Nonlinear Optical Effects in Molecules and Polymers*, Wiley, New York, **1991**.

[5] D. S. Chemla, J. Zyss, *Nonlinear Optical Properties of Organic Molecules and Crystals*, Academic Press, **1987**.

[6] a) S. Keinan, T. J. Marks, M. A. Ratner, *Chem. Mater.* **2004**, *16*, 1848; b) S. Di Bella, M. A. Ratner, T. J. Marks, *J. Am. Chem. Soc.* **1992**, *114*, 5842.

[7] a) K. Wu, J. G. Snijders, C. Lin, *J. Phys. Chem. B* **2002**, *106*, 8952; b) J. A. R. P. Sharma, J. L. Rao, K. Bhanuprakash, *Chem. Mater.* **1995**, *7*, 1843; c) L. Jensen, P.-O. Astrand, A. Osted, J. Kongsted, K. V. Mikkelsen, *J. Chem. Phys.* **2002**, *116*, 4001.

[8] a) J. Zyss, *J. Chem. Phys.* **1993**, *98*, 6583; b) J. Zyss, *Chem. Rev.* **1994**, *94*, 77.

[9] a) H. E. Katz, W. L. Wilson, G. Scheller, *J. Am. Chem. Soc.* **1994**, *116*, 6636; b) H. E. Katz, G. Scheller, T. M. Putvinski, M. L. Schilling, W. L. Wilson, C. E. D. Chidsey, *Science* **1991**, *254*, 1485.

[10] a) C. D. Gutsche, *Calixarenes Revisited*, Royal Society of Chemistry, Cambridge, **1998**. b) A. Ikeda, S. Shinkai, *Chem. Rev.* **1997**, *97*, 1713.

[11] a) M. S. Wong, X. L. Zhang, D. Z. Chen, W. H. Cheung, *Chem. Commun.* **2003**, 138; b) M. S. Wong, Z. H. Li, C. C. Kwok, *Tetrahedron Lett.* **2000**, *41*, 5719; c) T. Gu, C. Bourgogne, J.-F. Nierengarten, *Tetrahedron Lett.* **2001**, *42*, 7249.

[12] a) E. Kelderman, L. Derhaeg, G. J. T. Heesink, W. Verboom, J. F. J. Engbersen, N. F. van Hulst, A. Persoons, D. N. Reinhoudt, *Angew. Chem.* **1992**, *102*, 1107; *Angew. Chem. Int. Ed. Engl.* **1992**, *31*, 1075; b) F. Vocanson, P. S. Ferrand, R. Lamartine, A. Fort, A. W. Coleman, P. Shahgaldian, J. Mugnier, A. Zerroukhi, *J. Mater. Chem.* **2003**, *13*, 1596; c) T. Verbiest, S. Houbrechts, M. Kauranen, K. Clays, A. Persoons, *J. Mater. Chem.* **1997**, *7*, 2175.

[13] E. Brouyere, J. L. Bredas, *Synth. Met.* **1995**, *71*, 1699.

[14] P. D. J. Grootenhuis, P. A. Kollman, L. C. Groenen, D. N. Reinhoudt, G. J. van Hummel, F. Ugozzoli, G. D. Andreeti, *J. Am. Chem. Soc.* **1990**, *112*, 4165.

[15] A. S. Davydov, *Theory of Molecular Excitons*, McGraw-Hill, New York, **1962**.

[16] H. Suzuki, *Electronic Absorption Spectra: Geometry of Organic Molecules*, Academic Press, New York, **1967**.

[17] N. Harada, Y. Takuma, H. Uda, *J. Am. Chem. Soc.* **1978**, *100*, 4029.

[18] K. Nakanishi, *Circular Dichroic Spectroscopy: Exciton Coupling in Organic Stereochemistry*, University Science Books, Mill Valley, CA, **1983**.

[19] G. D. Scholes, K. P. Ghiggino, A. M. Oliver, M. N. Paddon-Row, *J. Am. Chem. Soc.* **1993**, *115*, 4345.

[20] J. McCullough, *Chem. Rev.* **1987**, *87*, 811; M. Kasha, *Rev. Mod. Phys.* **1959**, *31*, 162.

[21] a) A. Datta, S. K. Pati, *J. Chem. Phys.* **2003**, *118*, 8420; b) A. Datta, S. K. Pati, *J. Phys. Chem. A* **2004**, *108*, 320.

[22] a) J. A. Armstrong, N. Bloembergen, J. Ducuing, P. S. Pershan, *Phys. Rev.* **1962**, *127*, 1918; b) J. Ward, *Rev. Mod. Phys.* **1965**, *37*, 1; c) S. K. Pati, T. J. Marks, M. A. Ratner, *J. Am. Chem. Soc.* **2001**, *123*, 7287.

[23] A. D. Becke, *J. Chem. Phys.* **1993**, *98*, 1372.

[24] M. J. Frisch, M. Head-Gordon, J. A. Pople, *Chem. Phys. Lett.* **1990**, *166*, 281.

[25] James E. Huheey, E. A. Keiter, R. L. Keiter, *Inorganic Chemistry: Principles of Structure and Reactivity*, 4th ed., Pearson Education, **2000**.

[26] S. Scheiner, *Hydrogen Bonding. A Theoretical Perspective*, Oxford University Press, Oxford, **1997**.

[27] a) H. Sekino, R. J. Bartlett, *J. Chem. Phys.* **1986**, *85*, 976; b) V. Keshari, S. P. Karna, P. N. Prasad, *J. Phys. Chem.* **1993**, *97*, 3525.

[28] J. L. Oudar, D. S. Chemla, *J. Chem. Phys.* **1977**, *66*, 2664; J. L. Oudar, *J. Chem. Phys.* **1977**, *67*, 446.

[29] J. Ridley, M. C. Zerner, *Theor. Chim. Acta* **1973**, *32*, 111; A. D. Bacon, M. C. Zerner, *Theor. Chim. Acta* **1979**, *53*, 21.

[30] R. J. Buenker, S. D. Peyerimhoff, *Theor. Chim. Acta* **1974**, *35*, 33.

[31] Z. Shuai, D. Beljonne, J. L. Bredas, *J. Chem. Phys.* **1992**, *97*, 1132.

[32] D. Beljonne, Z. Shuai, J. Cornil, D. dos Santos, J. L. Bredas, *J. Chem. Phys.* **1999**, *111*, 2829.

[33] S. Ramasesha, Z. G. Soos, *Chem. Phys. Lett.* **1988**, *153*, 171; Z. G. Soos, S. Ramasesha, *J. Chem. Phys.* **1989**, *90*, 1067.

[34] S. Ramasesha, Z. Shuai, J. L. Bredas, *Chem. Phys. Lett.* **1995**, *245*, 224; I. D. L. Albert, S. Ramasesha, *J. Phys. Chem.* **1990**, *94*, 6540; S. Ramasesha, I. D. L. Albert, *Phys. Rev. B* **1990**, *42*, 8587.

[35] S. K. Pati, S. Ramasesha, Z. Shuai, J. L. Bredas, *Phys. Rev. B* **1999**, *59*, 14827.

[36] S. K. Pati, T. J. Marks, M. A. Ratner, *J. Am. Chem. Soc.* **2001**, *123*, 7287.

[37] F. H. Allen, S. Bellard, M. D. Brice, B. A. Cartwright, A. Doubleday, H. Higgs, T. Hummelink, B. G. Hummelink-Peters, O. Kennard, W. D. S. Motherwell, J. Rodgers, D. G. Watson, *Acta. Crystallogr. Sect. B* **1979**, *35*, 2331.

[38] K. Tsubaki, Y. Murata, K. Komatsu, T. Kinoshita, K. Fuji, *Heterocycles* **1999**, *51*, 2553.

[39] T. Yamato, F. Zhang, H. Tsuzuki, Y. Miura, *Eur. J. Org. Chem.* **2001**, 1069.

Received: November 25, 2004
Revised: March 23, 2005
Published online: June 23, 2005

